한국항해항만학회지 제48권 제2호
J. Navig. Port Res. Vol. 48, No. 2 : 125-136, April 2024 (ISSN:1598-5725(Print)/ISSN:2093-8470(Online))
DOI : http://dx.doi.org/10.5394/KINPR.2024.48.2.125

A Preliminary Study on Direct Ethanol SOFC for Marine Applications

Bo Rim Ryu · To Thi Thu Ha** · † Hokeun Kang*

,PhD. Student, Department of Marine System Engineering, Korea Maritime and Ocean University*
† Professor, Division of Coast Guard Studies, Korea Maritime and Ocean University

Abstract : *This research presents an innovative integrated ethanol solid oxide fuel cell (SOFC) system designed for applications in marine vessels. The system incorporates an exhaust gas heat recovery mechanism. The high-temperature exhaust gas produced by the SOFC is efficiently recovered through a sequential process involving a gas turbine (GT), a regenerative system, steam Rankine cycles, and a waste heat boiler (WHB). A comprehensive thermodynamic analysis of this integrated SOFC-GT-SRC-WHB system was performed. A simulation of this proposed system was conducted using Aspen Hysys V12.1, and a genetic algorithm was employed to optimize the system parameters. Thermodynamic equations based on the first and second laws of thermodynamics were utilized to assess the system's performance. Additionally, the exergy destruction within the crucial system components was examined. The system is projected to achieve an energy efficiency of 58.44% and an exergy efficiency of 29.43%. Notably, the integrated high-temperature exhaust gas recovery systems contribute significantly, generating 1129.1 kW, which accounts for 22.9% of the total power generated. Furthermore, the waste heat boiler was designed to produce 900.8 kg/h of superheated vapor at 170 ℃ and 405 kPa, serving various onboard ship purposes, such as heating fuel oil and accommodations for seafarers and equipment.*

Key words : *ethanol, SOFC, organic Rankine cycles, waste heat recovery, thermodynamics analysis*

1. Introduction

The maritime sector makes a substantial contribution to global air pollution, and this contribution is expected to grow as shipping activities increase(Xing et al., 2021). Reducing emissions from maritime vessels is imperative due to escalating environmental concerns, current emission constraints, and anticipated future regulations(Singh and Pedersen, 2016). Consequently, the International Maritime Organization(IMO) has introduced a series of stringent guidelines and regulations aimed at curbing both air pollution and greenhouse gas emissions (GHGs)(IMO, 2018; Hansson et al. 2020). The imperative need to develop energy sources that are both highly efficient and environmentally sustainable has become paramount in order to prevent lasting ecological harm for future generations. Within this context, there has been a significant focus on fuel cells and the concept of a hydrogen-based economy as promising advancements in energy systems that can facilitate more effective and eco-friendly energy generation. Fuel cells represent electrochemical devices that are free from the restrictions of the Carnot cycle, exhibiting theoretical efficiencies surpassing 80%. When hydrogen is employed as the fuel source, the only byproduct released into the atmosphere is water. Among the various types of fuel cells, SOFCs stand out as a technology with exceptional potential for converting chemical energy into electricity with remarkable efficiency. Consequently, SOFCs hold substantial promise for significantly reducing both fuel consumption and carbon dioxide(CO2) emissions. The utilization of SOFCs in maritime vessels has the potential to mitigate both acoustic and emission-related pollution stemming from ship exhaust, concurrently diminishing the noise originating from conventional diesel engines. In the early 19th century, Sir William Robert Grove pioneered the development of fuel cell technology, demonstrating its efficacy in harnessing the voltage generated by a battery to illuminate a lamp(Dhahad et al. 2020). In contrast to the strict fuel constraints imposed on many other types of batteries, solid oxide fuel cells(SOFCs) exhibit a wide range of flexibility and are considered one of the most economically viable energy storage devices ever developed, even in the presence of stringent pollution regulations. Moreover, to enhance its overall energy efficiency, SOFCs function as high-temperature fuel cells, thereby generating a significant amount of high-potential waste heat. Additionally, SOFCs possess the versatility to operate with various fuel sources and possess the capability to directly convert chemical energy into electricity(Cinti and Desideri, 2015).

† kkang@kmou.ac.kr 051-410-4260
* ruyborim@g.kmou.ac.kr

Nevertheless, a pivotal concern arises in the necessity to derive hydrogen from alternative primary sources. The majority of hydrogen is currently generated through the process of steam reforming of natural gas, which, in turn, necessitates the implementation of supplementary carbon capture technologies to achieve a fully carbon-neutral cycle. A biofuel combines the benefits of liquid fuels while also possessing a notably elevated energy density. Ethanol, among the array of biofuels available, stands out as the most extensively manufactured on a global scale and is likely the most mature biofuel, finding significant utility in the realm of transportation(Badwal et al. 2015; Gemes and De Bortoli, 2016).

Ethanol(CH3CH2OH) is a transparent, colorless liquid known by various names, including ethyl alcohol, grain alcohol, and EtOH. Irrespective of its origin, whether it comes from starch- or sugar-based sources like corn grain, sugar cane, or cellulosic materials, ethanol retains an identical chemical composition. Ethanol possesses a superior octane rating compared to gasoline, offering valuable blending characteristics. The mandated minimum octane number requirements for gasoline serve to prevent engine knocking and ensure smooth drivability. To achieve the standard 87 octane rating, lower-octane gasoline is blended with 10% ethanol. Ethanol serves as a domestically produced, renewable fuel for transportation. Whether employed in blends with lower ethanol content, including E10(90% gasoline, 10% ethanol), E15(ranging from 10.5% to 15% ethanol), or E85(a flex fuel blend comprising 51% to 83% ethanol, subject to geographic and seasonal variations), ethanol plays a significant role in mitigating emissions.

Nobrega et al.(2012) experimented with ethanol directly feeding to the SOFC in 100h, continuously, achieving a power output comparable to that attained when utilizing hydrogen. Electrochemical analyses revealed that within the anodic compartment, there is a gradual occurrence of internal steam reforming of ethanol derived from sugar cane, facilitated by the introduction of a remarkably catalytically active ceria-based layer onto the anode. Dogdibegovic et al.(2020) investigated the internal reforming of ethanol as fuel for SOFC under the Ni reforming catalyst. The disparity in performance between hydrogen and ethanol that has undergone full reforming can be ascribed solely to the reduction in hydrogen concentration. Notably, the SOFC exhibited a notably high peak power density under various conditions, such as achieving 1.0 W cm-2 at 650℃ when using an ethanol-water blend and anhydrous ethanol fuel obtain at 1.4Wcm^{-2} at 700℃. Preliminary durability assessments using an ethanol-water blend demonstrated promising stability, with the system sustaining operation for 100hours at 700℃ while maintaining a voltage of 0.7V. Importantly, there was no carbon deposition observed within the NiSDCN40 anode during its operation. Steil et al.(2017) experimented and analyzed direct ethanol supplying to the anode-supported SOFC. The nanostructured ceria-based catalyst establishes a uniform and porous layer, measuring 25mm in thickness, covering the Ni-based anode support. This layer does not exhibit any discernible impact on the operational performance of the fuel cell and effectively inhibits the formation of carbon deposits. Furthermore, this catalytic layer facilitates the steam reforming reactions of ethanol, leading to comparable current outputs when using both hydrogen and ethanol as fuels. The sustained stability of single cells, featuring relatively substantial active areas(8 cm^2), underscores the viability of employing a catalytic layer for the internal reforming of biofuels within SOFC.

Based on the literature review conducted above, ethanol proves as effective fuel for SOFC. Besides, because of the high-working temperature of SOFC, the utilization of waste heat recovery methodologies holds substantial potential for enhancing both the overall power output and performance of a system. However, the effectiveness of these bottoming cycles varies depending on the specific choice made for each one. The critical factor influencing the success of the system's design lies in the careful selection of appropriate integrating and bottoming cycles. Therefore, in this study, we propose the integration of the gas turbine - steam Rankine cycle(GT-SRC) and a waste heat boiler(WHB) with the primary system to effectively capture the high-temperature exhaust heat emanating from the SOFC. The specific research objectives and novelty of current research can be summarized as follows:

- Assessing the suitability of ethanol as a potential marine fuel to align with stringent environmental regulations at both local and international levels.
- Evaluating the suitability of ethanol SOFC as an excellent alternative for marine vessels, addressing the limitations of conventional Internal Combustion Engines (ICE).
- Developing and presenting a novel SOFC-GT-SRC-WHB integrated system tailored for use in existing marine vessels.
- Utilizing ASPEN Hysys V12.1 for the modeling of the

proposed system.

- Establishing comprehensive thermodynamic models of the system to predict key performance parameters, including power output, energy efficiency, and exergy efficiency.

The proposed system aims to offer a novel solution for marine vessels to adhere to environmental regulations. The selection of each combined and bottoming cycle has been made with careful consideration of factors such as operating conditions, available installation space, and user-friendliness for seafarers working onboard ships.

2. Materials and methods: System description

The entire system being studied has been designed for general cargo ships with a power capacity of 3,800kW, and it operates using ethanol as its fuel source. The specific details of the vessel can be detailly found in Table 1. The primary means of power generation in this system is the SOFC, which is responsible for driving the main propeller with a power output of 3,800kW.

Table 1 General information of ship particular

Items	Values
Propulsion type	Electric propulsion driving
Length overall	120m
Beam	13m
Electrical required	3800kW
Deadweight	3000 DWT

Fig. 1 presents an illustrative schematic diagram of the integrated SOFC-GT-SRC-WHB system using ethanol as the fuel source. The system begins with ethanol storage within the ethanol service tank, maintained at condition of 25℃ and 1 bar(Cordaro et al. 2023). Subsequently, the ethanol undergoes compression via a water pump and is pre-heated within the regeneration unit(HEX-3) to attain the necessary operating temperature for the fuel cells, reforming process, and pressure swing adsorption system. Water vapor(stream 6) generated during this process serves as the heat source for the ORC.

Air is introduced into the cathode of the SOFC after being pre-heated by the exhaust stream(stream 4) to achieve the requisite operating temperature for the SOFC. The exhaust gas produced during the electrochemical reaction within the SOFC is directed to the afterburner to complete the combustion process. This leads to the complete combustion of the exhaust gases emanating from both the cathode and anode of the SOFC, generating a substantial amount of heat and consequent temperature elevation. To maximize power output, the Gas Turbine (GT) and the bottoming cycles utilize the regenerators associated with the waste heat from the SOFC. Consequently, the waste heat is efficiently employed in a cascading manner to enhance system efficiency and performance.

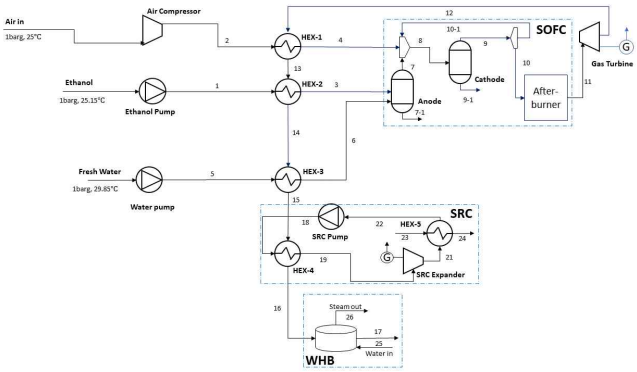

Fig. 1 Schematic of the SOFC-GT-SRC-WHB integrated system

The conversion of chemical energy into electricity generates a substantial amount of heat. This electrical output in the form of direct current is then converted into alternating current using an inverter(DC-AC), which is subsequently supplied to power the ship's propulsion system and other electrical components. Any unused portion of the ethanol and hydrogen mixture(stream 10-1) is reprocessed and combined with a fresh supply to enhance the efficiency and effectiveness of the SOFC. With increased heat production, the temperature continues to climb, guaranteeing the thorough combustion of the exhaust emissions from both the cathode and anode. The resulting high-temperature exhaust gas(stream 11) is then subjected to a gas turbine to produce mechanical power. The primary heat source for the SRC is derived from the waste heat originating from the SOFC through HEX-4. Initially, the water pressure within the SRC is increased by the SRC pump. Within the evaporator(HEX-4), the working fluid undergoes heating and vaporization, ultimately transforming into a superheated stream. The high-temperature steam (stream 19) is employed to drive a reversible heat pump after undergoing depressurization in the expander, thereby generating additional energy. The saturated water is subsequently condensed within the condenser HEX-5, and

this condensed water transfers heat to a fresh cooling water source.

To fulfill the needs of the ship's crew, who are required to remain onboard, the ship employs this water, which exits with a final temperature of 63.82℃ and a molar flow rate of 666.1 kgmole/h. In addition, the remaining waste heat from the SOFC(stream 16) is employed in a WHB to heat water (stream 25) and generate superheated vapor. The steam produced by the waste heat boiler serves various purposes, including lubricating oil systems, air conditioning, and heating onboard the ship.

3. Models and methods

3.1 Thermodynamic model assumptions

In this subsection, we delve into the thermodynamic equations that pertain to the systems described, encompassing aspects such as mass and energy balances, energy dissipation rates, and entropy balances. We employ methodologies that assess both energetic and exergetic performance to facilitate comprehensive thermodynamic modeling and analysis. Furthermore, several factors are taken into account when assessing thermal performance from a thermodynamic perspective. These fundamental assumptions underpin our model:

The system as a whole operates under steady-state conditions.

Variations in the system's kinetic and potential energy are not taken into consideration.

Heat losses to the environment through pipe connections are deemed negligible.

Pressure drops within the pipelines are not factored into the analysis.

3.2 Model of the SOFC

In this research, the SOFC is modeled using the four elements of kinetic electrochemical reactions, electron transport, ionic, charge balancing, and heat transfer. The foundation for SOFC power generation is electrochemical reactions involving hydrogen and oxygen.

Reforming reaction

General:

$$C_2H_5OH + H_2O \leftrightarrow 4H_2 + 2CO \qquad \triangle h^0_{298K} = 255.7KJ/mol_{4H_2} \tag{1}$$

Decomposition reaction:

$$C_2H_5OH \rightarrow CH_4 + H_2 + CO \tag{2}$$

Water gas shift:

$$CO + H_2O \leftrightarrow H_2 + CO_2 \tag{3}$$

$$2H_2 \leftrightarrow 4H^+ + 4e^- \tag{4}$$

Electrochemical:

$$O_2 + 4e^- + 4H^+ \rightarrow 2H_2O \tag{5}$$

$$O_2 + 2H_2 \rightarrow 2H_2O \tag{6}$$

The Steam-to-Carbon ratio (STCR):

$$STCR = \frac{q_{H_2O}}{q_{Ethanol}} \tag{7}$$

Fuel and oxidant utilization

The utilization of ethanol can be assessed by analyzing the real-world provision and consumption of this fuel or its hydrogen counterpart(Zhou et al. 2022; Zheng et al. 2022):

$$U_{fuel} = \frac{Ethanol_{reacted}}{Ethanol_{supply}} \tag{8}$$

Air utilization:

$$U_{air} = \frac{Ethanol_{reacted}}{Ethanol_{supply}} \tag{9}$$

The mass flow rate of required ethanol and air supply:

$$q_{fuel} = \frac{i \cdot N_{Cell} \cdot A_{Cell}}{U_f \cdot n_e \cdot F}\left(\frac{mol}{s}\right) \tag{10}$$

The amount of required hydrogen can be estimated by:

$$m_{SOFC,\ hydrogen} = 2 \cdot m_{SOFC,Oxygen}\left(\frac{mol}{\min}\right) \tag{11}$$

The output power of stack of SOFC(Song et al, 2021; Liu et al. 2019; Chitgar and Moghimi, 2020):

$$W_{stack} = i.A.V_c\eta_{DA} \tag{12}$$

where and are represent for the current density(A/m^2), area of cell surface(m^2), actual voltage value(Vc) and DC-AC converter efficiency, respectively(Liu et al. 2019; Ezzat and Dincer, 2020).

The current density(i) is estimated by:

$$i = \frac{z.F.n_e}{N_{cell}\ A} \tag{13}$$

The Vc is calculated by:

$$V_c = V_R - \quad V_{loss} \tag{14}$$

in which represents ideal reversible voltage and, stands for voltage loss.

$$V_{loss} = V_{ohm} + V_{act} + V_{con} \tag{15}$$

where, is the ohmic losses(V), denote the concentration losses(V) and denote activation losses(V).

$$V_{ohm} = V_{ohm,a} + V_{ohm,c} + V_{ohm,e} + V_{ohm,int} \tag{16}$$

$$V_{ohm,a} = \frac{i\rho_a(A\pi D_m)}{8t_a} \tag{17}$$

$$V_{ohm,a} = \frac{i\rho_a(A\pi D_m)}{8t_a} A(A + 2(1 - A - B)) \tag{18}$$

$$V_{ohm,e} = i\rho_a t_e \tag{19}$$

$$V_{ohm,int} = i.\ \rho_{int}.\pi.\ D_m \frac{t_{int}}{w_{int}} \tag{20}$$

$$V_{act} = \frac{2RT}{F.\ n_e}\ Arcsinh\left(\frac{i}{2i_{0,k}}\right) \tag{21}$$

$$V_{con} = \frac{RT}{2F} ln\left(\frac{1 - \frac{i}{i_{L,H_2}}}{1 + \frac{i}{i_{L,O_2}}}\right) + \frac{RT}{2F} ln\left(\frac{1}{1 - \frac{i}{i_{L,O_2}}}\right) \tag{22}$$

Besides, the I-V curve is also widely employed to estimate the cell stack voltage(Fuerte et al. 2009; Al-Hamed and Dincer, 2021; Ma et al. 2006).

SOFC's energy efficiency of SOFC:

$$\eta_{en,\ SOFC} = \frac{\dot{W}_{elect,SOFC}}{\dot{m}_1 h_1 + \dot{m}_2 h_2 - \dot{m}_{11} h_{11}} \tag{23}$$

Or(Liu et al. 2019; Mehrpooya et al. 2015):

$$\eta_{en,SOFC} = \frac{\dot{W}_{SOFC}}{\dot{m}_1 \bullet LHV_{Ethanol}} \tag{24}$$

where denotes the mass flow rate of Ethanol supplied to the SOFC(kg/h) and stands for low heating value of Ethanol(kJ/kg).

Afterburner

The surplus fuel and air remaining from the electrochemical process in the SOFC can be continuously combusted in an afterburner to elevate the gas turbine's inlet temperature and pressure(Eveloy et al. 2016):

$$O_2 + 2CO \rightarrow 2CO_2 \tag{25}$$

$$O_2 + 2H_2 \rightarrow 2H_2O \tag{26}$$

3.3 GT

As the heated gaseous blend enters the gas turbine from the afterburner, it undergoes expansion, leading to the production of valuable mechanical energy. This process affects the exhaust temperature of the gas turbine:

$$T_{out} = T_{in}(PR)^{\frac{(k-1)}{k}} \tag{27}$$

in which, and $R = \frac{P_{in}}{P_{out}}$ and $k = \frac{\sum y_i \dot{\overline{C}}_{p,i}}{\sum y_i \overline{C}_{v,i}}$

Isentropic efficiency:

$$\eta_{s,T} = \frac{\sum(\dot{n}_i \overline{h}_i)_{in} - \sum(\dot{n}_i \overline{h}_i)_{out}}{\sum(\dot{n}_i \overline{h}_i)_{in} - \sum(\dot{n}_i \overline{h}_i)_{s,out}} \tag{28}$$

Exergy efficiency:

$$\psi_T = \frac{\dot{W}_T}{\sum(\dot{n}_i \overline{ex}_i)_{in} - \sum(\dot{n}_i \overline{ex}_i)_{out}} \tag{29}$$

SOFC-GT subsystem:

Energy efficiency:

$$\eta_{en,SOFC,GT} = \frac{\dot{W}_{SOFC} + \dot{W}_{GT}}{\dot{m}_1\ LHV_{Ethanol}} \tag{30}$$

Exergy efficiency:

$$\eta_{ex,SOFC,GT} = \frac{\dot{W}_{SOFC} + \dot{W}_{GT}}{\dot{m}_1\ ex_{Ethanol}} \tag{31}$$

Air compressor

The isentropic efficiency:

$$\eta_{en,Compressor} = \frac{\sum(\dot{n}_i \overline{h}_i)s,_{out} - \sum(\dot{n}_i \overline{h}_i)_{in}}{\sum(\dot{n}_i \overline{h}_i)_{out} - \sum(\dot{n}_i \overline{h}_i)_{in}} \tag{32}$$

The exergy efficiency:

$$\eta_{ex,Compressor} = \frac{\sum(\dot{n}_i \overline{ex}_i)_{in} - \sum_i(\dot{n}_i \overline{ex}_i)_{out}}{\dot{W}_C} \quad (33)$$

Electric generator

The powers of the electric generator:

$$\dot{W}_G = \eta_G(\dot{W}_T - \dot{W}_C) \quad (34)$$

Heat exchangers

The hot and cold streams of the heat exchanger:

Hot and cold streams:

$$\dot{Q} = \sum(\dot{n}_i \bar{c}_{p,i})_h (T_{h,in} - T_{h,out}) \quad (35)$$

$$\dot{Q} = \sum(\dot{n}_i \bar{c}_{p,i})_h (T_{c,in} - T_{c,out}) \quad (36)$$

3.4 SRC

The energy balance of SRC's turbine:

$$\dot{m}_{wf,SRC} h_{20} = \dot{W}_{SRC,T} + \dot{m}_{wf,SRC} h_{21} \quad (37)$$

The net power output:

$$\dot{W}_{\neq t,SRC} = \dot{W}_{SRC,\mathrm{Expander}} - \dot{W}_{SRC\ Pump} \quad (38)$$

Efficiencies:

$$\eta_{en,SRC} = \frac{\dot{W}_{elec,SRC}}{\dot{m}_{15}(h_{15} - h_{16})} \quad (39)$$

$$\eta_{ex,SRC} = \frac{\dot{W}_{elec,SRC}}{\dot{m}_{15}(ex_{15} - ex_{16})} \quad (40)$$

3.5 Waste heat boiler

Functioning akin to a heat exchanger, the WHB utilizes heat derived from the flue gas to produce steam within the boiler drum. The inflow of high-temperature exhaust gas into the WHB is quantified at 8113kg/h at a temperature of 224.4℃. As a result of this process, superheated steam is generated, with the steam reaching conditions of 170℃, 405 kPa, and a flow rate of 50kgmole/h(equivalent to 900.8 kg/h).

The total heat transfer by the WHB(Barelli et al. 2020):

$$Q = U \cdot A \cdot LMTD \quad (41)$$

where LMTD is the logarithmic mean temperature difference, U is the heat exchange coefficient, and A is the heat exchange area(m^2).

$$LMTD = \frac{\triangle T_{2,end} - \triangle T_{1,end}}{\ln\left(\frac{\triangle T_{2,end}}{\triangle T_{1,end}}\right)} \quad (42)$$

where temperature between hot and cold source at the

Table 2 The exergy destruction in the major components

Components	Exergy destruction rate	
SOFC	$\dot{E}x_1 + \dot{E}x_2 + \dot{E}x_{10-1} - \dot{E}x_{10} - \dot{W}_s = \dot{E}x_{des}$	(43)
Afterburner	$\dot{E}x_{10} - \dot{E}x_{11} = \dot{E}x_{des}$	(44)
Gas Turbine	$\dot{E}x_{11} - \dot{E}x_{12} - \dot{W}_{Gas\ turbine} = \dot{E}x_{des}$	(45)
HEX-1	$\dot{E}x_2 + \dot{E}x_{12} - \dot{E}x_4 - \dot{E}_{13} = \dot{E}x_{des}$	(46)
HEX-2	$\dot{E}x_1 + \dot{E}x_{13} - \dot{E}x_3 - \dot{E}_{14} = \dot{E}x_{des}$	(47)
HEX-3	$\dot{E}x_5 + \dot{E}x_{14} - \dot{E}x_6 - \dot{E}_{15} = \dot{E}x_{des}$	(48)
HEX-4	$\dot{E}x_{15} + \dot{E}x_{18} - \dot{E}x_{19} - \dot{E}_{16} = \dot{E}x_{des}$	(49)
HEX-5	$\dot{E}x_{21} + \dot{E}x_{23} - \dot{E}x_{22} - \dot{E}_{24} = \dot{E}x_{des}$	(50)
WHB	$\dot{E}x_{16} + \dot{E}x_{25} - \dot{E}x_{17} - \dot{E}x_{26} = \dot{E}x_{des}$	(51)
SRC Expander	$\dot{E}x_{19} - \dot{E}x_{21} - \dot{W}_{S_{Turbine}} = \dot{E}x_{des}$	(52)

ends of heat exchanger.

Table 2 lists the exergy destruction rates for the primary components.

The performance of integrated system can be calculated as Al-Hamed and Dincer(2021), Gholamian and Zare(2016), Meng et al.(2022).

Energy efficiency:

$$\eta_{\frac{en,}{all}} = \frac{\dot{W}_{elec,system}}{\dot{m}_{Ethanol} LHV_{Ethanol}} \quad (53)$$

where is the net power generation and consumed of the described system:

$$\dot{W}_{elec,total} = \dot{W}_{elec,SOFC} + \dot{W}_{turbine} + \dot{W}_{SRC,turbine} - \dot{W}_{Aircomp} - \dot{W}_{SRC,pump} \quad (54)$$

$LHV_{Ethanol}$ is lower heating value of Ethanol(kJ/kg).

Exergy efficiency:

$$\eta_{\frac{ex,}{all}} = \frac{\dot{W}_{elec,total}}{\dot{m}_{Ethanol} ex_{Ethanol}} \quad (55)$$

4. Materials and methods:

The proposed system of ethanol SOFC-GT-SRC-WHB is modelled by ASPEN-HYSYS V12.1(Aspen Technology Inc, US)(Lee, 2019; Song and Gu, 2015). The simulation software employed REFPROP as Aspen Physical Property System(Razmi and Janbaz, 2020). The ethanol SOFC-GT-SRC-WHB system underwent simulation and thermodynamic assessment by the Peng-Robinson equation of state to delineate the thermodynamic conditions of the stream compositions and parameters.

To streamline the thermodynamic analysis of the system, the following standard assumptions were employed:

- The air supplied is at condition of 25.15℃ and 101.3 kPa.
- The ambient air comprises 21% oxygen(O_2) and 79% nitrogen(N_2).

Table 3 displays the simulated boundary conditions(Ezzat and Dincer, 2020; Al-Hamed and Dince, 2021).

5. Materials and methods: Modeling verification

Table 4 displays a comparison between the primary parameters generated in our current study and the data provided in a previous work by Liu et al.(2019). Our calculated values closely align with the literature data, and the discrepancies between the two datasets fall within acceptable limits.

By employing the waste heat boiler in the suggested manner, the superheated stream may be used to alter

Table 3 The design and working indicators of system

Component	Parameter	Unit	Value
-	Number of single cells	-	18,471
-	Operating Temperature	℃	862.3
-	Active surface area	m^2	0.2
-	Fuel cell current density	A/m^2	1432
-	Operating Pressure	bar	4.01
-	Electrolyte thickness	cm	0.01
-	Anode thickness	cm	0.002
-	Fuel utilization factor in SOFC	-	85%
-	Cathode thickness	cm	0.002
Converter	DC-AC converter efficiency	%	98
Expanders	Isentropic efficiency	%	88
Compressor and Pumps	Isentropic efficiency	%	85

demands from sailors' quarters, heat lubricating oil, warm up, etc. Additionally, the SRC may generate hot water from its condenser while also powering the ship's propulsion engine and other electronic equipment. The waste heat recovery subsystem has demonstrated its requirement by producing 30.08% of total generated electricity.

6. Results and discussions

6.1 The performances of system

The targeted vessel is equipped with electric power propulsion systems requiring 3800kW to facilitate main propeller operation, maneuvering procedures, auxiliary machinery, and meet the energy demands of the crew on board. The assessment outcomes indicate that the SOFC exhibits a cell voltage of 0.733V and an energy efficiency of 50.2%. Subsequently, the combined system's power output, assessed using the thermodynamic model detailed in previous section, is estimated to be 4929.1kW. This combined system harnesses a variety of power sources, including waste heat cycles.

Notably, the subsystems contribute 22.9% of the total power output, while the SOFC accounts for the remaining 77.1%. These results affirm the operational success of the described system according to the initial plan. In addition to propelling the main propeller, the total power generated is sufficient to meet the additional electrical needs for auxiliary applications.

The energy and exergy efficiencies of overall system are estimated at 58.44% and 29.43%, respectively.

The SRC demonstrated its performance with 28.12% and 51.29% of energy and exergy efficiency, respectively. Energy efficiency of total system increased by 8.24% when waste heat from SOFC was recovered by SRC as opposed to SOFC alone.

A study of the exergy degradation rates associated with the internal thermal processes occurring in the system's key components is shown in Figure 3. The uppermost three exergy destruction rates of 2905.1kW, 1819.99kW and 864.26 kW counted for the SOFC, GT and Afterburner, respectively. A major source of irreversible electrochemical reaction is responsible for the biggest SOFC exergy destruction. Given the high rate of energy loss, the gas turbine has more space for development than other machinery components. The fourth is belonging to SRC expander with its values of 560.9kW. Among the heat exchangers, the HEX-3 presented highest exergy destruction rate with value of 395.55kW. The differential between hot and cold sources made up the high value of exergy destruction.

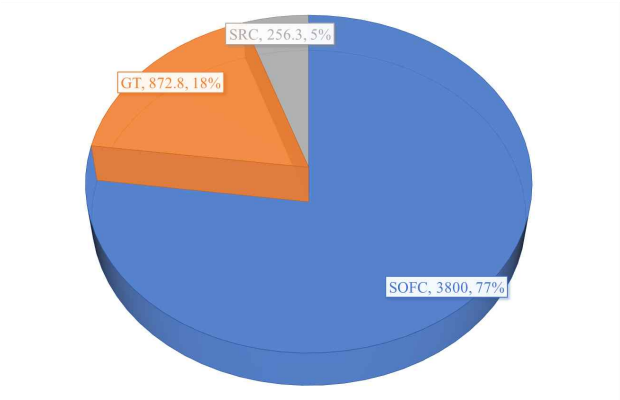

Fig. 2 Power produced by major components

Table 5 Performance of major subsystem

Subsystem	Energy efficiency (%)	Exergy efficiency (%)
SOFC	50.20	-
SOFC-GT	55.19	27.79
SRC	28.12	51.29
Total system	58.44	29.43

Due to the efficient heat transfer between the water in the economizer and the flue gas, WHB may destroy 329.9 kW of energy. This different in WHB caused by it is employing both of energy utilization from fresh water supply and waste heat recovery of high temperature exhaust gas. The follow exergy destruction is belonging to HEX-2, HEX-4 and HEX-5 with 223.45kW, 94.77kW and 55.34kW, respectively. The SOFC exhaust gas's source was utilized in the evaporator of SRC and transferred to usable power output.

Table 6 presents the detailly of thermodynamic points of each node.

Table 4 The outcomes of the simulation conducted using the integrated model are presented alongside the pertinent variables obtained from the analysis of Liu et al.(2019)

Parameter	Modelling	Literature	
		Reported (Liu et al., 2019)	Different
SOFC temperature(°C)	862.3	870	0.88%
Gas Turbine inlet temperature(°C)	1173	1201	2.33%
Cell voltage(V)	0.733	0.747	1.87%
Current Density(A/m^2)	1432	1429	0.2%
SOFC efficiency	50.2	50.96	0.72%

Table 6 The design and working indicators of system

	Vapour Fraction	Temperature (℃)	Pressure (kPa)	Molar Flow (kgmole/h)	Mass Enthalpy (kJ/kg)
1	0.00	25.23	420.00	21.99	-6052.13
Ethanol	0.00	25.15	101.33	21.99	-6052.67
Fresh water	0.00	29.85	101.00	56.23	-15866.90
Air in	1.00	29.85	101.30	210.99	4.63
2	1.00	311.07	400.00	210.99	297.67
3	1.00	427.00	416.55	21.99	-4284.14
4	1.00	427.00	396.55	210.99	423.28
5	0.00	29.88	480.00	56.23	-15866.40
6	1.00	250.00	473.11	56.23	-13003.51
7	1.00	216.85	416.55	86.62	-8643.86
8	1.00	371.28	396.55	316.34	-1840.96
9	1.00	862.28	396.55	374.67	-1840.97
10	1.00	862.28	396.55	355.94	-1840.97
11	1.00	1173.49	396.55	347.75	-1840.95
12	1.00	934.53	128.00	347.75	-2228.26
13	1.00	875.11	121.11	347.75	-2322.50
14	1.00	733.70	114.21	347.75	-2543.25
15	1.00	496.80	79.74	347.75	-2900.72
16	1.00	224.40	72.84	347.75	-3290.00
17	0.97	45.39	72.84	347.75	-3595.14
18	0.00	72.12	19000.00	75.49	-15667.37
19	1.00	360.90	18996.55	75.49	-13345.07
20	1.00	360.90	18996.55	75.49	-13345.07
21	0.70	74.69	38.00	75.49	-14023.43
22	0.00	70.00	31.11	75.49	-15693.37
23	0.00	20.00	100.00	666.11	-15909.39
24	0.00	63.82	96.55	666.11	-15720.13
25	0.00	20.00	405.00	50.00	-15909.10
26	1.00	170.00	405.00	50.00	-13160.74

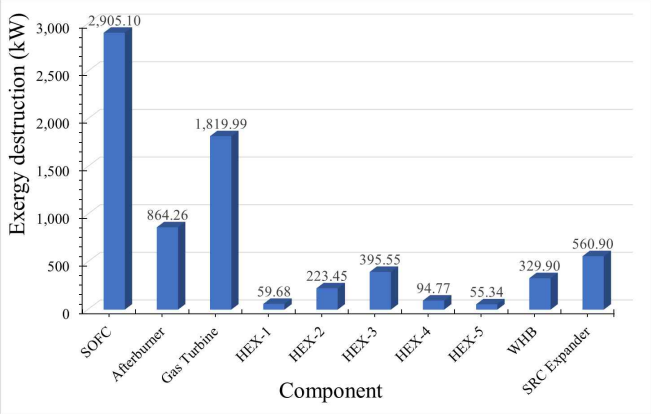

Fig. 3 Exergy destruction of major components

7. Conclusions

This research proposed and investigated a system that utilizes ethanol as the primary fuel source and incorporates a combination of SOFC-GT-SRC-WHB components to generate electricity for the primary propulsion system of maritime vessels. This intergenerational energy system aims to offer environmentally sustainable options for marine vessels by utilizing renewable, sulfur-free, and low-carbon fuels in power generation. The performance of the suggested system has been assessed through energy and exergy calculations, along with extensive parametric investigations. Key conclusions drawn from this research include:

The integrated system exhibits a total energy and exergy efficiency of 58.44% and 29.43%, respectively, when compared to stand-alone SOFC systems. Furthermore, the GT-SRC-WHB subsystem contributes 1129.1kW, constituting 22.9% of the overall power supply of the system.

The waste heat boiler demonstrates the capability to meet various onboard heating requirements, including lubricating oil, machinery, and crew accommodations, by generating 900.8kg/h of superheated vapor at 170℃ and 405 kPa.

These findings suggest the feasibility of developing highly efficient SOFC-GT-SRC-WHB marine propulsion systems fueled by ethanol. Further research considerations should explore the practical applications of this integrated system in various maritime contexts.

Acknowledgement

This research is the winner of the Marine Fisheries Future Risk Paper Contest sponsored by the Korea Maritime Institute(KMI).

This research was supported by "Development and demonstration of ammonia fueled engine for medium/large sized vessels" funded by the Ministry of Trade, Industry and Energy(MOTIE, Korea) (RS-2023-00285272).

References

[1] Al-Hamed, K. H. M. and Dincer, I.(2021), "A novel ammonia solid oxide fuel cell-based powering system with on-board hydrogen production for clean locomotives", Energy, Vol. 220, doi: 10.1016/j.energy.2021.119771.

[2] Badwal, S. P. S., Giddey, S., Kulkarni, A., Goel, J. and Basu, S.(2015), "Direct ethanol fuel cells for transport and stationary applications - A comprehensive review," Applied Energy, Vol. 145, pp. 80-103, doi: 10.1016/j.apenergy.2015.02.002.

[3] Barelli, L., Bidini, G. and Cinti, G.(2020), "Operation of a solid oxide fuel cell based power system with ammonia as a fuel: Experimental test and system design", Energies, Vol. 13, No. 23, doi: 10.3390/en13236173.

[4] Chitgar, N. and Moghimi, M.(2020), "Design and evaluation of a novel multi-generation system based on SOFC-GT for electricity, fresh water and hydrogen production", Energy, Vol. 197, doi: 10.1016/j.energy.2020.117162.

[5] Cinti. G. and Desideri, U.(2015), "SOFC fuelled with reformed urea", Applied Energy, Vol. 154, pp. 242-253, doi: 10.1016/j.apenergy.2015.04.126.

[6] Cordaro, P. G., Braga, B. L., Corotti, D., Gallego, A. G. and Silveira, J. L.(2023), "Electricity and hydrogen production by cogeneration system applied in a fuel station in Brazil: Energy analysis of a combined SOFC and ethanol steam reforming model", Fuel, Vol. 356, doi: 10.1016/j.fuel.2023.129615.

[7] Dhahad, H. A., S. Ahmadi, H. A., Dahari, M., Ghaebi,H. and Parikhani, T.(2020), "Energy, exergy, and exergoeconomic evaluation of a novel CCP system based on a solid oxide fuel cell integrated with absorption and ejector refrigeration cycles", Thermal Science and Engineering Progress, Vol. 21, pp. 100755,

doi: 10.1016/j.tsep.2020.100755.

[8] Dogdibegovic, E., Fukuyama, Y. and Tucker, M. C.(2020), "Ethanol internal reforming in solid oxide fuel cells: A path toward high performance metal-supported cells for vehicular applications", Journal of Power Sources, Vol. 449, pp. 1-25, doi: 10.1016/j.jpowsour.2019.227598.

[9] Eveloy, V., Rodgers, P. and Qiu, L.(2016), "Integration of an atmospheric solid oxide fuel cell - gas turbine system with reverse osmosis for distributed seawater desalination in a process facility", Energy Conversion and Management, Vol. 126, pp. 944-959, doi: 10.1016/j.enconman.2016.08.026.

[10] Ezzat, M. F. and Dincer, I.(2020), "Energy and exergy analyses of a novel ammonia combined power plant operating with gas turbine and solid oxide fuel cell systems", Energy, Vol. 194, doi: 10.1016/j.energy.2019.116750.

[11] Fuerte, A., Valenzuela, R. X., Escudero, M. J. and Daza, L.(2009), "Ammonia as efficient fuel for SOFC", Journal of Power Sources, Vol. 192, No. 1, pp. 170-174, doi: 10.1016/j.jpowsour.2008.11.037.

[12] Gholamian E. and Zare, V.(2016), "A comparative thermodynamic investigation with environmental analysis of SOFC waste heat to power conversion employing Kalina and Organic Rankine Cycles", Energy Conversion and Management, Vol. 117, pp. 150-161, doi: 10.1016/j.enconman.2016.03.011.

[13] Gomes. R. S. and De Bortoli, A. L.(2016), "A three-dimensional mathematical model for the anode of a direct ethanol fuel cell," Applied Energy, Vol. 183, pp. 1292-1301, doi: 10.1016/j.apenergy.2016.09.083.

[14] Hansson, J., Brynolf, S., Fridell, E. and Lehtveer, M.(2020), "The potential role of ammonia as marine fuel-based on energy systems modeling and multi-criteria decision analysis" Sustainability, Vol. 12, No. 8, pp. 10-14, doi: 10.3390/SU12083265.

[15] International Maritime Organzation(2018), Adoption of the Initial IMO Strategy on Reduction of GHG Emissions from Ships.

[16] Lee, Y. H.(2019), "Thermo-economic analysis of a novel regasification system with liquefied-natural-gas cold-energy", International Journal of Refrigeration, Vol. 101, pp. 218-229, doi: 10.1016/j.ijrefrig.2019.03.022.

[17] Liu, Y., Han, J. and You, H.(2019), "Performance analysis of a CCHP system based on SOFC/GT/CO2 cycle and ORC with LNG cold energy utilization", International Jounal of Hydrogen Energy, Vol. 44, No. 56, pp. 29700-29710, doi: 10.1016/j.ijhydene.2019.02.201.

[18] Ma, Q., Peng, R. R., Tian, L. and Meng, G.(2006), "Direct utilization of ammonia in intermediate-temperature solid oxide fuel cells", Electrochem. commun., Vol. 8, No. 11, pp. 1791-1795, doi: 10.1016/j.elecom.2006.08.012.

[19] Mehrpooya, M., Dehghani, H. and Ali Moosavian, S. M.(2015), "Optimal design of solid oxide fuel cell, ammonia-water single effect absorption cycle and Rankine steam cycle hybrid system", Journal of Power Sources, Vol. 306, pp. 107-123, doi: 10.1016/j.jpowsour.2015.11.103.

[20] Meng, T., Cui, D., Ji, Y., Cheng, M. and Tu, B.(2022), "ScienceDirect Optimization and efficiency analysis of methanol SOFC-PEMFC hybrid system", International Jounal of Hydrogen Energy, doi: 10.1016/j.ijhydene.2022.06.102.

[21] Nobrega, S. D., Galesco, M. V., Girona, K., de Florio, D. Z., Steil, M. C., Georges, S. and Fonseca, F. C.(2012), "Direct ethanol solid oxide fuel cell operating in gradual internal reforming," J. Power Sources, Vol. 213, pp. 156-159, doi: 10.1016/j.jpowsour.2012.03.104.

[22] Razmi, A. R. and Janbaz, M.(2020), "Exergoeconomic assessment with reliability consideration of a green cogeneration system based on compressed air energy storage (CAES)", Energy Conversion and Management, Vol. 204, doi: 10.1016/j.enconman.2019.112320.

[23] Singh, D. V. and Pedersen, E.(2016), "A review of waste heat recovery technologies for maritime applications," Energy Conversion and Management, Vol. 111, pp. 315-328, doi: 10.1016/j.enconman.2015.12.073.

[24] Song, M., Zhuang, Y., Zhang, L., Li, W., Du, J. and Shen, S.(2021), "Thermodynamic performance assessment of SOFC-RC-KC system for multiple waste heat recovery", Energy Conversion and Management, Vol. 245, doi: 10.1016/j.enconman.2021.114579.

[25] Song, J. and wei Gu, C.(2015), "Performance analysis of a dual-loop organic Rankine cycle (ORC) system with wet steam expansion for engine waste heat recovery", Applied Energy, Vol. 156, pp. 280-289, doi: 10.1016/j.apenergy.2015.07.019.

[26] Steil, M. C., Nobrega, S. D., Georges, S., Gelin, P., Uhlenbruck, S. and Fonseca, F. C.(2017), "Durable direct ethanol anode-supported solid oxide fuel cell", Applied Energy, Vol. 199, pp. 180-186, doi: 10.1016/j.apenergy.2017.04.086.

[27] Xing, H., Stuart, C., Spence, S. and Chen, H.(2021), “Alternative fuel options for low carbon maritime transportation: Pathways to 2050,” Journal of Cleaner Production, Vol. 297, doi: 10.1016/j.jclepro.2021.126651.

[28] Zhou, J., Wang, Z., Han, M., Sun, Z. and Sun, K.(2022), “Optimization of a 30 kW SOFC combined heat and power system with different cycles and hydrocarbon fuels”, International Jounal of Hydrogen Energy, Vol. 47, No. 6, pp. 4109-4119, doi: 10.1016/j.ijhydene.2021.11.049.

[29] Zheng, N., Duan, L., Wang, X., Lu, Z. and Zhang, H.(2022), “Thermodynamic performance analysis of a novel PEMEC-SOFC-based poly-generation system integrated mechanical compression and thermal energy storage”, Energy Conversion and Management, Vol. 265, doi: 10.1016/j.enconman.2022.115770.

Received 02 November 2023
Revised 08 February 2024
Accepted 08 February 2024